

# Self-similar Tilings Based on Prototiles Constructed from Segments of Regular Polygons

Robert W. Fathauer  
Tessellations  
Tempe, AZ 85281, U.S.A.  
E-mail: tessella@futureone.com

## Abstract

Two infinite families of self-similar tilings are described which have apparently not been reported before. Each tiling is based on a single prototile that is a segment of a regular polygon. Each tiling is also edge to edge and bounded in the Euclidean plane, by means of the tiles being reduced in size by a fixed scaling factor. This results in self similarity. Tilings are constructed from these prototiles that are of a rich visual complexity, and an example is given of an Escher-like design based on one of these tilings.

## 1. Introduction

Tiling is a topic in which math and art combine wonderfully. While the rigorous mathematical treatment of tiling is beyond the understanding of the average person, anyone can appreciate the beauty of tilings. While the best-behaved tilings fill the infinite Euclidean plane, infinite tilings can also be finite in area by means of the tiles becoming infinitesimally small at the boundaries. In many cases, the boundaries of these tilings are fractal, which adds another element of beauty to them.

The sorts of tilings dealt with here are not to be confused with hyperbolic tilings. In the latter, hyperbolic geometry is used to depict an infinite tiling in, for example, the Poincaré disk. In such tilings, the individual tiles appear distorted in Euclidean space, which is how we perceive the world. In the tilings discussed in this paper the tiles are not distorted, but are all of the same shape (in mathematical terminology “similar”).

The Dutch graphic artist M.C. Escher explored bounded tilings, but he only executed a single finished print of the general sort described here, namely “Square Limit” [1]. His other prints depicting bounded tilings, the four “Circle Limit” prints, are based on hyperbolic geometry. He also made several prints based on unbounded tilings in which the tiles become infinitesimally small at the center.

Others have worked on non-hyperbolic bounded tilings since Escher [2-5]. In almost all of these tilings, the prototile has two long edges, so that three or more of these tiles meet in a point at the center of the tiling. The resultant tilings have  $n$ -fold rotational symmetry, with  $n \geq 3$ .

In this paper, two families of tilings are presented in which, in their simplest form, the center is a line shared by two identical tiles that possess a single long edge. The tilings thus possess 2-fold rotational symmetry. The prototiles are constructed from segments of regular polygons. In the first family, the prototiles are isosceles triangles, while in the second they are trapezoids. The simple forms of these tilings are combined and modified to make more complex tilings of greater esthetic appeal. These families of tilings do not appear to have been reported before.

Figure 1 illustrates the construction of the prototiles from regular polygons. In the first family, denoted “s” tilings, the tiles are triangular and are generated by connecting two vertices

encompassing two adjacent edges. In the second family, denoted “u” tilings, the tiles are trapezoidal and are generated by connecting two vertices encompassing three adjacent edges. The tilings are constructed by reducing these prototiles by a scaling factor given by the ratio of the short to long edges of the prototile, and then matching the long edges of the next smaller generation to the short edges of the larger generation. The simplest starting point for constructing a bounded tiling is to place two of the largest-generation tiles back to back. This process is illustrated in Figure 2.

## 2. s Tilings

Overlapping of tiles is not allowed in any reasonably well-behaved tiling, which restricts the allowed values of  $s$ . This is clarified in Figure 3 for two different values of  $s$ . It is readily apparent through experimentation that this condition restricts the allowed generating regular polygons to those with number of sides  $n = 4, 6, 8, 10, \dots$ . The triangular prototile generated from a polygon with  $n$  sides is simply referred to as the “ $s = n$  prototile”. These triangles are isosceles, with the two identical angles given by  $\pi/s$ . The linear reduction factor from a given prototile to the next smaller generation of prototile is given by  $1/(2(\cos(\pi/s)))$ .

The simplest bounded infinite tiling for a given prototile is denoted the “pod” for that prototile. The pods for  $s = 4, 6, 8, 10$ , and  $12$  are shown in Figure 4. (In all of the figures, the tilings are constructed through a finite number of generations adequate to illustrate the general appearance of the infinite tiling.) All of these have fractal boundaries except for  $s = 4$ , for which the boundary is an octagon in which four sides are of one length and the other four of a second length  $\sqrt{2}$  times the first length.

Note that there are two distinct types of vertices that are intrinsic to these tilings. The first type, marked “A” in Figure 4 is the point at which the tip (the point at which the two short edges meet) of a triangle meets the bases of  $n + 2$  smaller triangles. The second type, marked “B” in Figure 4 is the point at which the tips of two triangles meet the bases of 4 smaller triangles. The point marked “C” indicates a third type of vertex that results from the choice of putting two large tiles back to back. It is possible to construct tilings without vertices of type C, as well as to create other types of vertices by construction choices. Only types A and B are always present, and there is an infinite number of each type in any tiling. Each pod possesses 2-fold rotational symmetry about its center and two axes of mirror symmetry.

Pods can be joined to form more complex tilings. The two basic configurations for joining pods that result in bounded tilings are denoted “rings” and “stars”. Some examples of rings and stars based on  $s$  pods are shown in Figure 5. These have been restricted to those tilings that are edge to edge. This means that only certain numbers of pods can be combined in rings and stars for a given value of  $s$ . Pods can also be joined in periodic fashion to extend over the infinite Euclidean plane.

An even greater degree of complexity can be introduced in these tilings by “perforating” the pods. This refers to removal of the largest generation of tiles in the pods, followed by filling in of the resultant hole with tiles of the same and smaller size as the remaining tiles. This process is illustrated in Figure 6. A tiling obtained in this way is shown in Figure 7. Note that perforated stars and rings are equivalent to more complex combinations of unperforated pods.

An Escher-like design based on the  $s = 6$  tiling is shown in Figure 8, where the triangular tile has been modified and detailing added to suggest a bird motif. The prototiles have been arranged in such a way that half the birds are flying left to right, and half right to left.

### 3. $u$ tilings

Again, the tilings are restricted to those values of  $u$  for which the tiles do not overlap. It is apparent from experimentation with  $u$  tilings that this condition restricts the allowed generating regular polygons to those with number of sides  $n = 6, 10, 14, 18, \dots$ . The trapezoidal prototile generated from a polygon with  $n$  sides is similarly referred to as the  $u = n$  prototile. The prototiles have three sides of equal length, with the two small angles in the trapezoid given by  $2\pi/u$ . The linear reduction factor from a given prototile to the next smaller generation of prototile is given by  $1/(1 + 2(\cos(2\pi/u)))$ .

The pods for  $u = 6, 10$ , and  $14$  are shown in Figure 9. All of these have fractal boundaries except for  $u = 6$ , for which the boundary is a regular hexagon. There are two distinct types of intrinsic vertices for  $u$  tilings as well. Type "A" is a point at which a tip of a trapezoid meets the bases of  $u/2 + 1$  smaller tiles. Type "B" is a point at which the tips of two trapezoids meet the bases of 2 smaller tiles. Each pod again possesses 2-fold rotational symmetry about its center and two axes of mirror symmetry.

The  $u$  pods can also be combined to form more complex tilings. Two examples of rings and stars based on  $u$  pods are shown in Figure 10. Perforation of  $u$  pods is carried out in a similar fashion to that used for  $s$  pods. A perforated star is also shown in Figure 10.

Additional prototiles can of course be constructed from regular polygons by connecting vertices encompassing more than three edges. However, it can be shown that none of these allow well-behaved tilings.

### 4. Conclusion

Two new families of self-similar tilings have been demonstrated in which the prototile is a segment of a regular polygon. In the first family the prototiles are isosceles triangles, while they are trapezoids in the second family. The tilings constructed from these prototiles look quite different from most bounded tilings presented previously. There are an infinite number of distinct prototiles in each family, and tilings can be constructed from these prototiles that are of a rich visual complexity.

### References

- [1] *The Magic Mirror of M.C. Escher*, by Bruno Ernst (Ballantine Books, New York, 1976).
- [2] Robert W. Fathauer, *Extending Recognizable-motif Tilings to Multiple-solution Tilings and Fractal Motifs*, to be published in the Proceedings of the Centennial Escher Congress, held in Rome and Ravello in June of 1998.
- [3] Peter Raedschelders, private communication. Examples can be seen on Mr. Raedschelders web site, <http://home.planetinternet.be/~praedsch/index.htm>.
- [4] Chaim Goodman-Strauss, private communication. Prof. Goodman-Strauss has constructed a number of tilings in which each tile is a fractal object related to the Koch snowflake.
- [5] Robert W. Fathauer, presented at the 1999 Bridges Conference (Winfield, Kansas, August 1999).

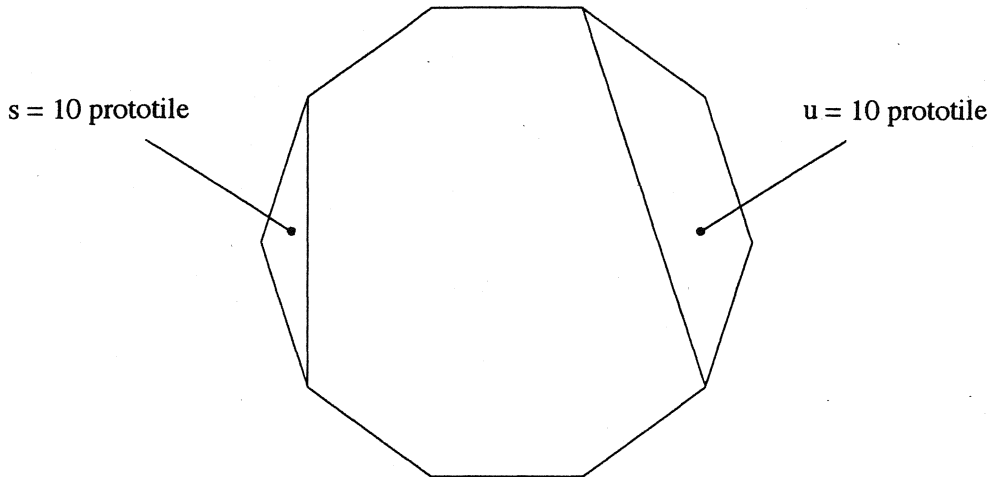


**Figure 1:** Construction of the  $s$  and  $u$  prototiles from a regular polygon, for the case of a regular decagon.

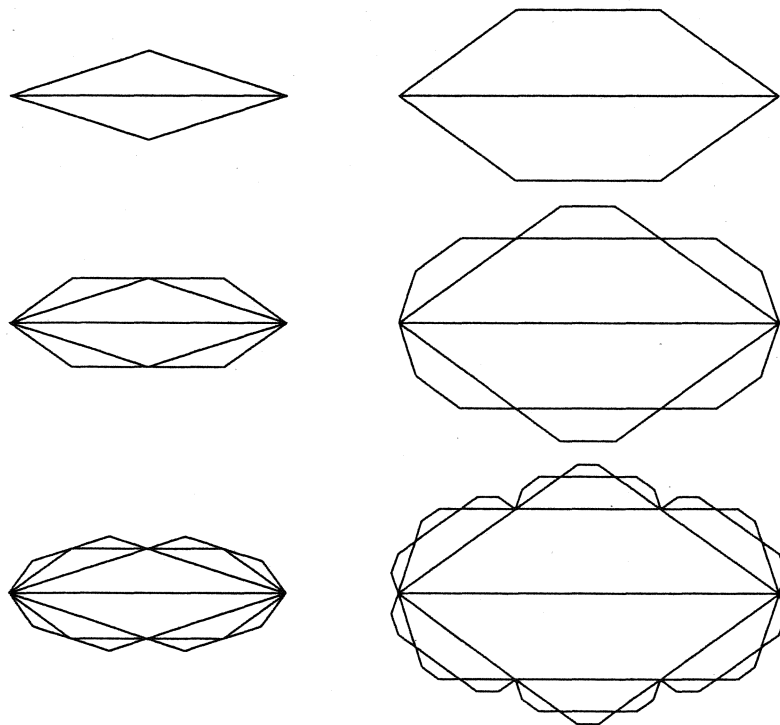


**Figure 2:** The first three steps in the construction of the simplest bounded infinite tilings based on the  $s$  and  $u$  prototiles.

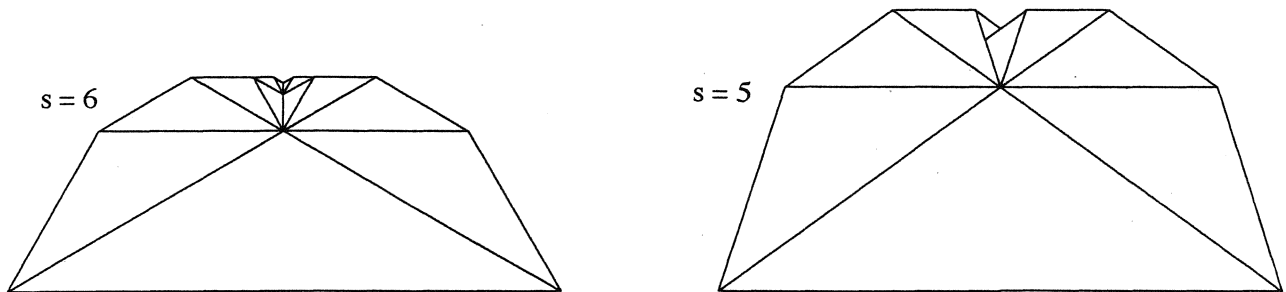


**Figure 3:** A portion of two  $s$  tilings illustrating how the tilings fold in upon themselves. Note that the first case,  $s = 6$ , is well behaved, while the second case,  $s = 5$ , is not. The tiles overlap in the second case, which is not allowed.

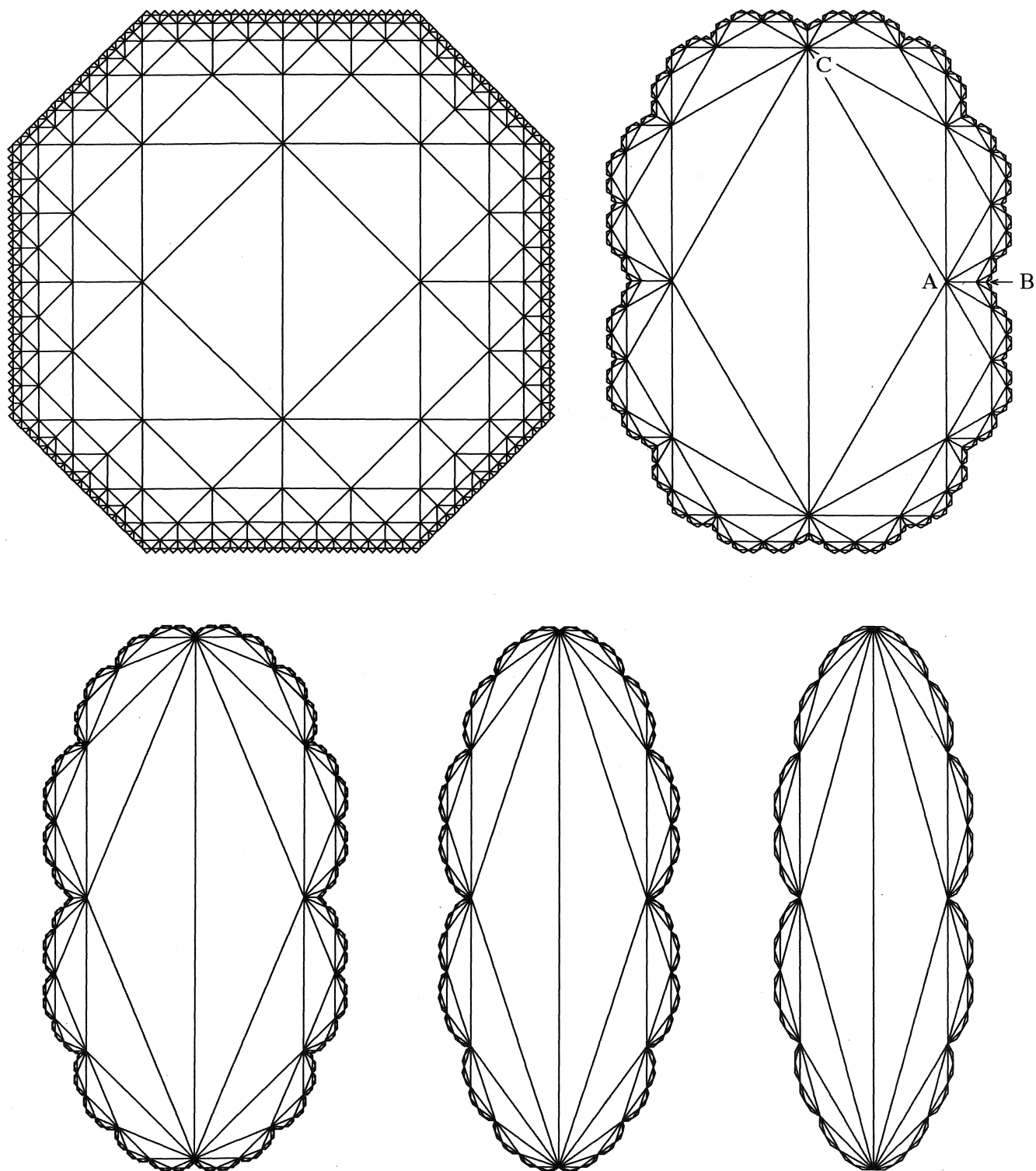
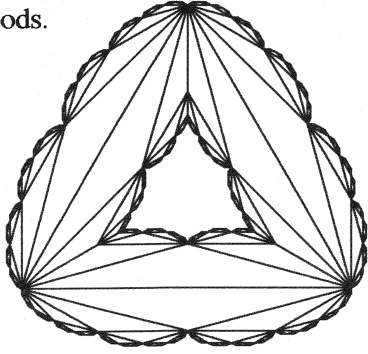
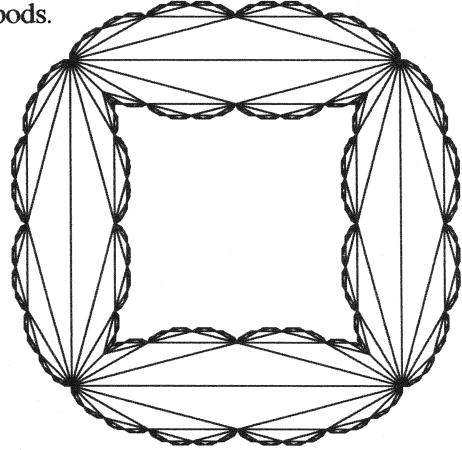


**Figure 4:** Pods for  $s = 4, 6, 8, 10,$  and  $12$ . The points  $A, B,$  and  $C$  on the  $s = 6$  pod mark the three different types of vertices that occur.

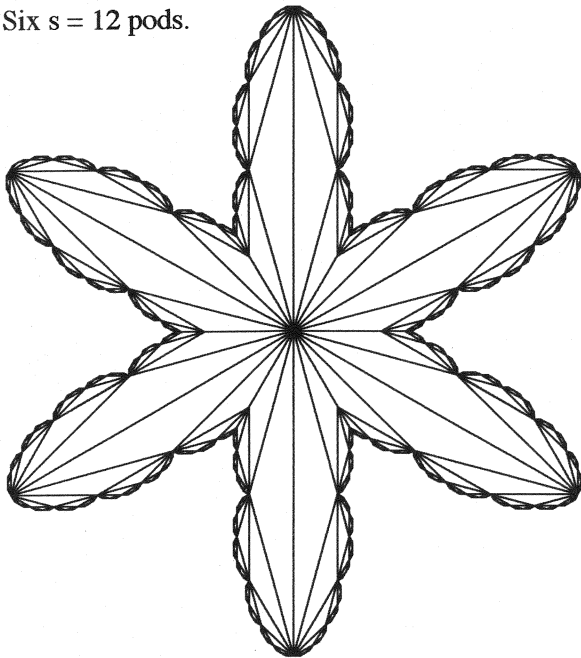
Three  $s = 12$  pods.



Four  $s = 12$  pods.



Six  $s = 12$  pods.



Twelve  $s = 12$  pods.

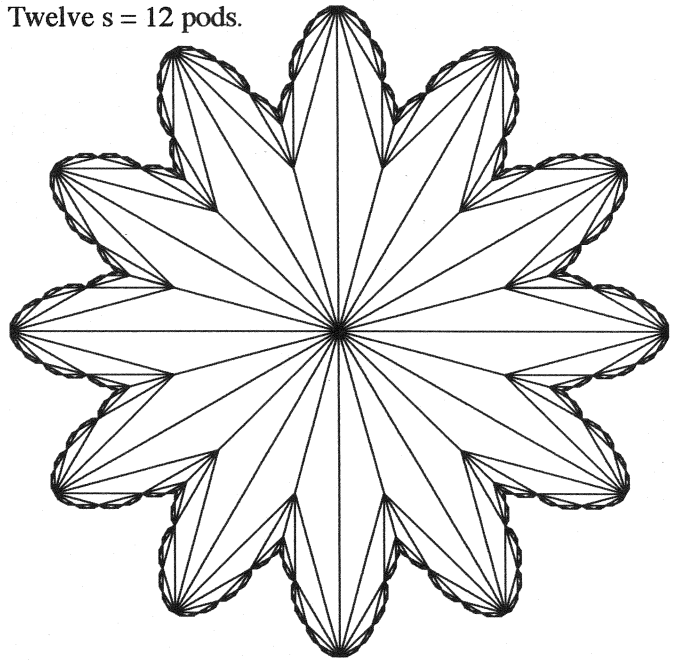


**Figure 5:** Two rings and two stars based on  $s = 12$  pods.

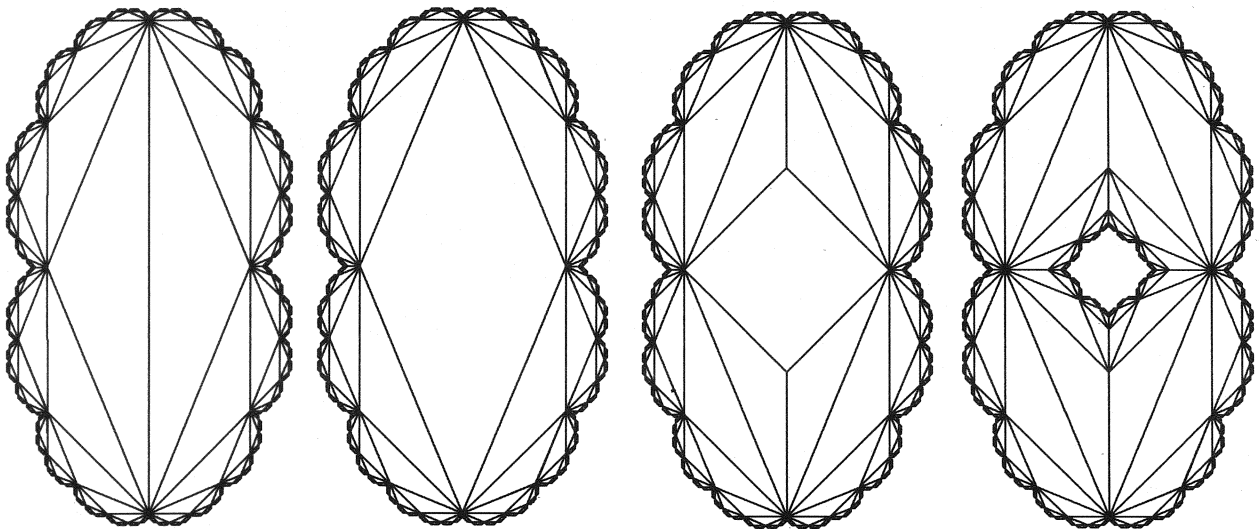


**Figure 6:** The process by which a pod is perforated.

**Figure 7:** A ring of four  $s = 8$  pods, perforated three times.

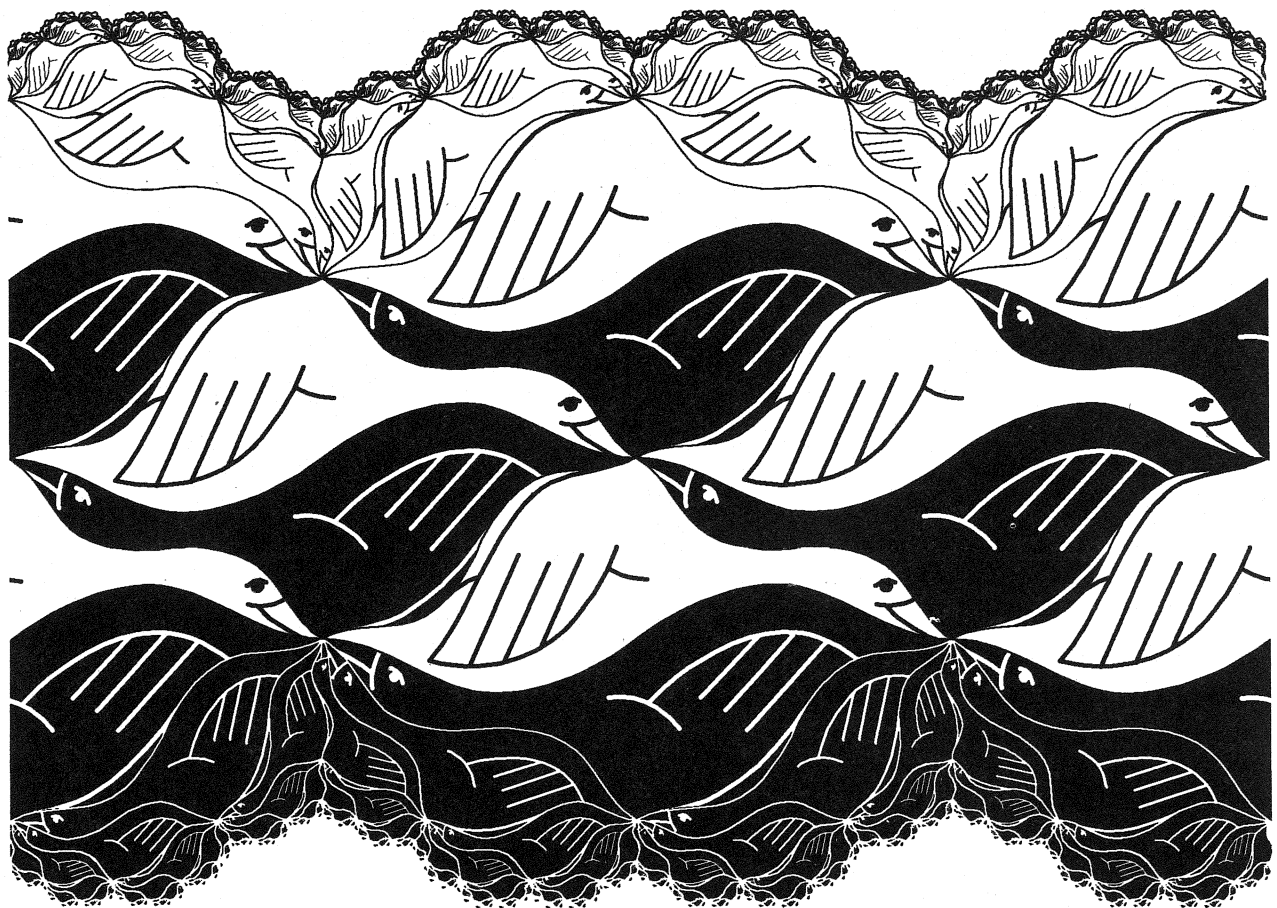
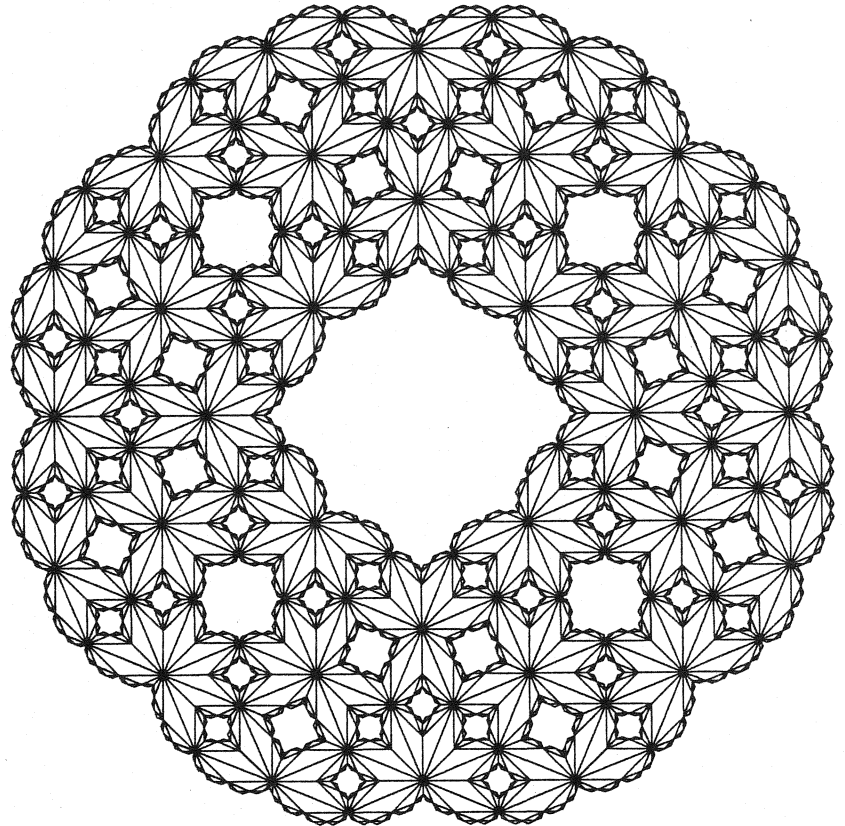


**Figure 8:** An Escher-like design based on an  $s = 6$  tiling.

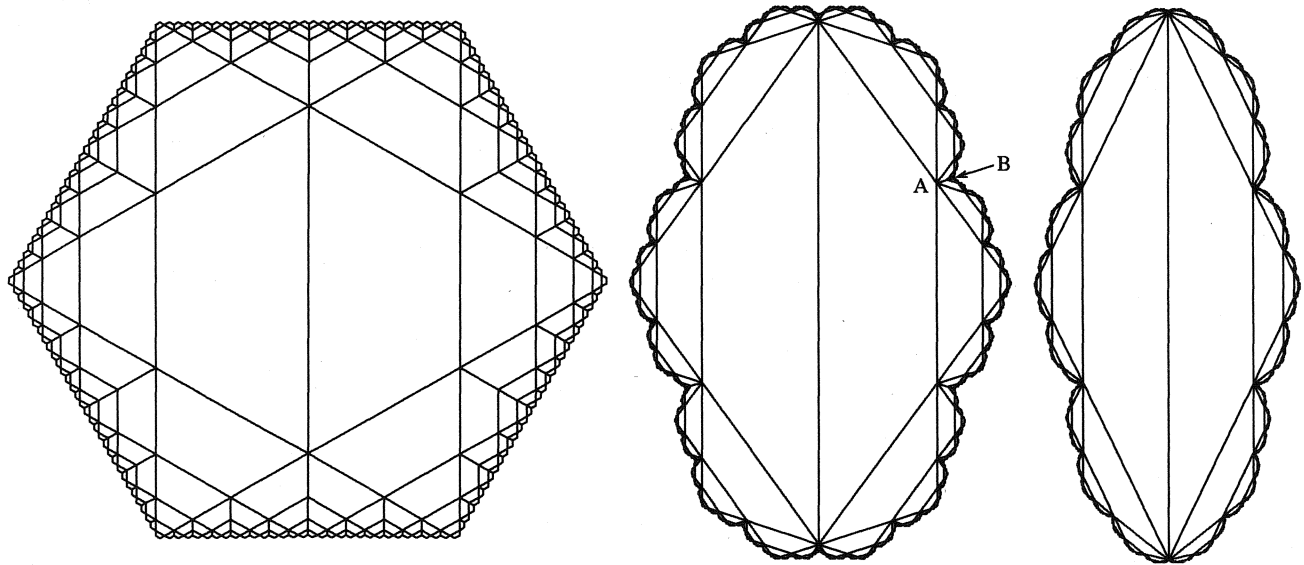


**Figure 9:** Pods for  $u = 6, 10,$  and  $14$ . The points  $A$  and  $B$  illustrate the two types of vertices intrinsic to  $u$  tilings.

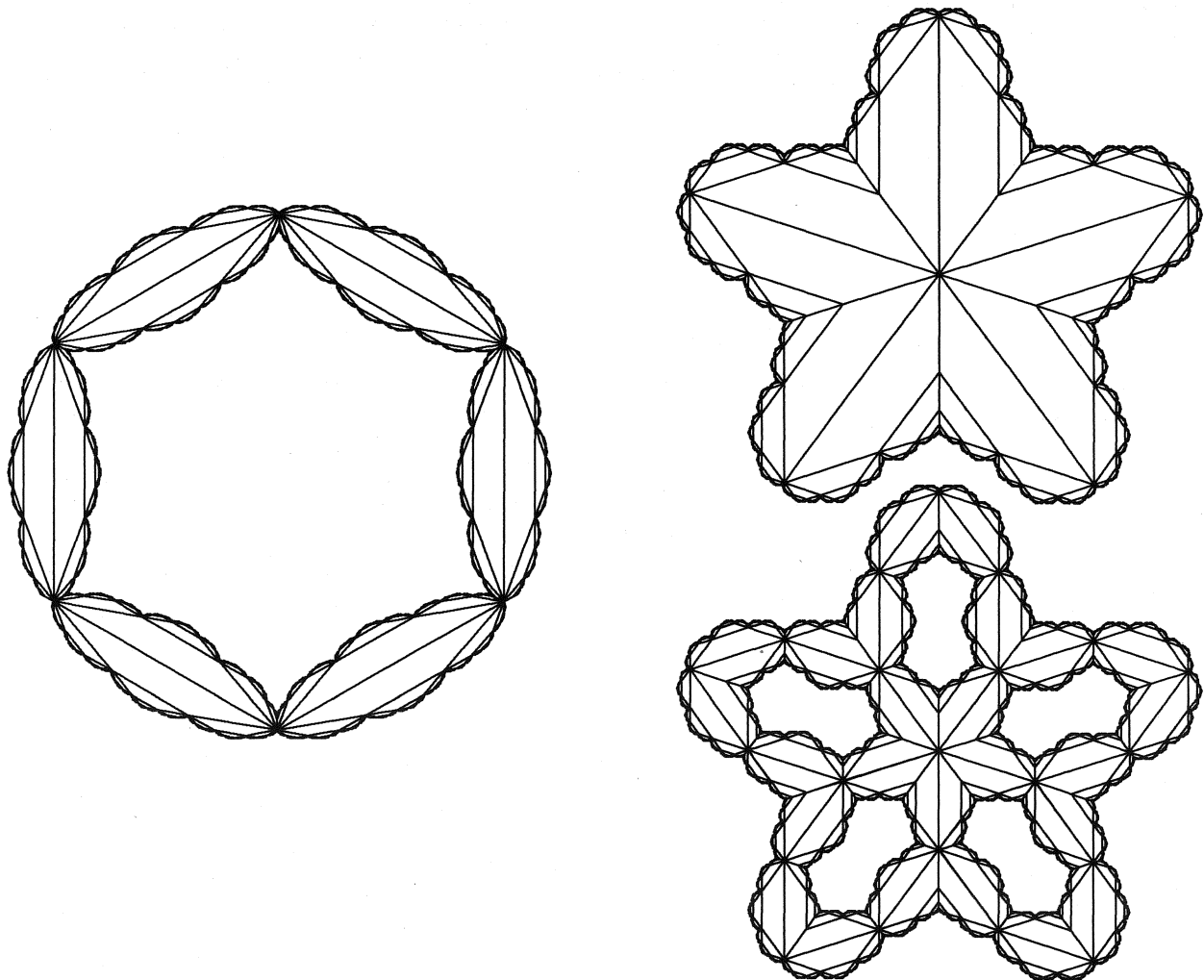


**Figure 10:** A ring formed from six  $u = 18$  pods, a star formed from five  $u = 10$  pods, and the same star perforated once.